Cancer Chemother Pharmacol (2017) 79:843–853
DOI 10.1007/s00280-017-3290-0

ORIGINAL ARTICLE

# Genotoxicity kinetics in murine normoblasts as an approach for the in vivo action of difluorodeoxycytidine

**Pedro Morales-Ramírez[1] · Teresita Vallarino-Kelly[1] · Virginia Cruz-Vallejo[1]**

Received: 12 October 2016 / Accepted: 14 March 2017 / Published online: 21 March 2017


**Abstract**
*Purpose* This study analyzed the kinetics of in vivo micronucleus induction in normoblasts by determining the kinetics of difluorodeoxycytidine (dFdC)-induced micronucleated polychromatic erythrocytes (MN-PCEs) in the peripheral blood of mice. The kinetic indexes of MN-PCE induction of dFdC were correlated with the previously reported mechanisms DNA damage induction by this compound. In general, this study aimed to establish an in vivo approach for discerning the processes underlying micronucleus induction by antineoplastic agents or mutagens in general.
*Methods* The frequencies of PCEs and MN-PCEs in the peripheral blood of mice were determined prior to treatment and after treatment using dFdC at doses of 95, 190, or 380 μmol/kg at 8 h intervals throughout a 72 h post-treatment.
*Results* The area beneath the curve (ABC) for MN-PCE induction as a function of time, which is an index of the total effect, indicated that the dose response was directly proportional and that the effect of dFdC on micronucleus induction was reduced compared with that of aneuploidogens and monofunctional and bifunctional alkylating agents but increased compared with that of promutagens, which is consistent with our previous results. The ABC showed a single peak with a small broadness index, which indicates that dFdC has a single mechanism or concomitant mechanisms for inducing DNA breaks. The time of the relative maximal induction ($T_{rmi}$) indicated that dFdC requires more time to achieve MN-PCE induction compared with aneugens and monofunctional and bifunctional alkylating agents, although it requires a similar time to achieve MN-PCE induction as azacytidine, which is consistent with evidence showing that both agents must be incorporated into DNA for their action to be realized. The timing of maximal cytotoxicity observed with the lowest dFdC dose was correlated with the timing of the main genotoxic effect. However, early and late cytotoxic effects were detected, and these effects were independent of the genotoxic response.
*Conclusions* A correlation analysis indicated that dFdC appears to induce MN-PCEs through only one mechanism or mechanisms that occur concomitantly, which could be explained by the previously reported concurrent inhibitory effects of dFdC on DNA polymerase alpha, polymerase epsilon, and/or topoisomerase. The timing of maximal cytotoxicity was correlated with the timing of maximal genotoxicity; however, an early cytotoxic effect that appeared to occur prior to the incorporation of dFdC into DNA was likely related to a previously reported inhibitory effect of dFdC on thymidylate synthase and/or ribonucleotide reductase.

**Keywords** Micronuclei · Cytotoxicity · Erythrocytes · DNA breaks · In vivo

✉ Pedro Morales-Ramírez
mordep1@yahoo.com.mx

Teresita Vallarino-Kelly
teresita.vallarino@inin.gob.mx

Virginia Cruz-Vallejo
virginia.cruz@inin.gob.mx

[1] Instituto Nacional de Investigaciones Nucleares, Apartado Postal 18-1027, Mexico City, Mexico

## Introduction

Antineoplastic agents act by altering processes related to cell proliferation, thereby causing cell death. Specifically,

these agents alter nucleotide metabolism [1], DNA structure [2], and DNA function after incorporation [3], repair [4], methylation [5], or mitotic cell division [6].

In particular, base analog antimetabolites alter various processes in a complex manner as observed in previous in vitro studies. To confirm these observations, the effects of therapeutic importance must be determined under conditions similar to the in vivo treatment conditions. The in vitro effects of these agents might vary from the in vivo effects, particularly when differences in the effective concentration and time of exposure and the complexity of the in vivo systems are observed. These findings provide evidence that the effectiveness of difluorodeoxycytidine (dFdC) in vivo is markedly lower than its effectiveness in vitro because of several factors [7].

Based on the hypothesis that the timing of DNA break induction in normoblasts depends on the operative mechanisms and should be reflected in the kinetics of the micronucleated polychromatic erythrocyte (MN-PCE) frequency in peripheral blood [8], we developed an alternative method to correlate the kinetics of the induction of micronuclei in murine peripheral blood in vivo with the in vitro mechanisms of action previously reported in cells. In addition, a cytotoxic-kinetic analysis was conducted by measuring the reduction in young erythrocytes caused by cell death or a delay in cell division during erythropoiesis [9].

Based on our previous studies, the time of relative maximal induction ($T_{rmi}$) index was developed, and it represents the difference between the timing of maximal MN-PCE induction caused by chemical agents and the timing of maximal induction caused by gamma rays [9]. Using this index, we were able to correlate the timing of DNA break induction with the kinetics of micronuclei induction. Gamma rays were used as a reference, because they directly induce lesions, thus allowing us to discard the duration of the general erythroblast enucleation process, which takes several hours. $T_{rmi}$ was used to discriminate between the following three categories: aneuploidogens, which exhibited a low $T_{rmi}$ of $3.5 \pm 1.4$ h; monofunctional and bifunctional alkylating agents, which showed a $T_{rmi}$ of $6.5 \pm 0.6$ h; and alkylating agents, which require metabolic activation in the liver and presented a $T_{rmi}$ of $14.3 \pm 0.8$ h. Two agents did not fit into these groups: the alkylating agent methylnitrosourea (MNU) ($T_{rmi}$ of 11.5 h), because lesions caused by this agent were falsely interpreted as mismatches that subsequently induced DNA breaks [10] and azacytidine (azaC) ($T_{rmi}$ of 9.5 h), likely because this agent has a complex mechanism of action which depends on its incorporation to DNA [9]. These results obtained with doses that cause a cytotoxic response that was 23–57% of the maximal PCE reduction, suggests a good correlation between the $T_{rmi}$ index and certain aspects of antineoplastic agent action. The study of the kinetics of MN-PCE induction by other antineoplastic base analogs that are dependent on prior incorporation into DNA would confirm whether the action of these antimetabolite agents occurs at a different time. This correlation would allow us to establish a predictive kinetic analysis to determine that effects involved in the therapeutic action of an antineoplastic agent to select agents with antineoplastic potential and infer the possible mechanisms of action of genotoxic agents in general.

In addition, kinetic analyses allow for the establishment of a strong index of the mutagenic effect by measuring the area beneath the curve (ABC) of MN-PCE induction vs time and an index of genotoxic capacity (GC) that correlates the ABC with the dose in μmoles per kg of body weight. Similarly, the cytotoxic capacity (CC), which relates the maximal cytotoxicity (percentage) with the dose in μmol/kg, is determined. A previous report indicated that dFdC increases the frequency of MN-PCEs and reduces the frequency of PCEs in murine bone-marrow cells and showed that these effects are not proportional to the dose [11].

The aims of this study were to (i) determine the kinetics of in vivo micronuclei induction by dFdC via the kinetics of MN-PCE induction in the peripheral blood of mice, (ii) correlate these kinetics with the reported genotoxic and cytotoxic actions of this agent, and (iii) determine the genotoxic and cytotoxic efficiencies of dFdC.

## Materials and methods

### Protocol

Groups of five mice were treated with single dFdC doses of 95, 190, or 380 μmoles per kg of body weight (corresponding to 25, 50, and 100 mg/kg, respectively). The dose range was selected based on previously obtained data for mice [12, 13]. The doses used in the present study represent 7.5, 15, and 30% of the lethal dose of 333 mg/kg [14].

Blood samples were obtained from the tail of each animal prior to the treatment and every 8 h after treatment up to 72 h. The kinetics of the genotoxic action were established by scoring the frequency of MN-PCEs per 2000 PCEs in each animal prior to exposure and every 8 h until 72 h post-treatment. The area under the curve of the MN-PCEs vs time, which was used as an index of total MN-PCE induction, and the timing of maximal induction after administering the different doses of dFdC was also determined and compared with those obtained for previously studied agents. The cytotoxicity was determined by scoring the number of PCEs per 2000 erythrocytes at various times, and the degree of cytotoxicity was determined based on the lowest frequency of PCEs observed at different times after exposure. The basal MN-PCE and PCE frequencies

obtained prior to exposure (0 h) were used as control values.

### Animals

Two-to-three-month-old male BALB/c mice weighing approximately 30 g were used in this study. The animals were maintained and bred in our laboratory under controlled temperature (22 ± 2 °C) and 12 h dark/12 h light cycle conditions. The mice were provided Purina chow for small rodents and water ad libitum.

### Treatments

After dilution, dFdC (Gemzar, Eli Lilly Co., Indianapolis, IN, USA) was intraperitoneally administered in 0.1 ml of water at doses of 95, 190, or 380 µmol per kg of body weight.

### Slides

Four samples were obtained from each mouse at each timepoint. Smears were prepared by adding a drop of blood obtained by either cutting a small segment of the tail or transferring a blood clot to a drop of fetal calf serum on a slide. The dried smears were stained using the May–Grunwald–Giemsa technique [15] and then mounted in resin.

#### *MN-PCE and PCE scoring*

The frequency of MN-PCEs per 2000 PCE erythrocytes was determined for each mouse belonging to each group ($n = 5$). The cells were scored according to the following criteria: (i) round morphology; (ii) diameter equal to 1/20th to 1/5th of the erythrocyte diameter; and (iii) deep purple color after staining. As mentioned in "Results", fewer than 2000 PCEs were used to determine the MN-PCE frequency at certain timepoints because of the level of dFdC cytotoxicity. For the same samples, the frequencies of PCEs per 2000 erythrocytes were determined.

### Kinetics of MN-PCE induction

The kinetics of MN-PCE induction were established based on the MN-PCE frequency over time [16]. The data obtained from each animal were plotted as the cumulative frequency (%) of MN-PCEs per 2000 PCEs as a function of time. These graphs were adjusted to a Boltzmann sigmoid curve on a PC using the following equation:

$$y = A_2 + (A_1 - A_2)/\{1 + \exp[(x - x_o)/dx$$

where $A_1$ is the initial frequency of MN-PCEs; $A_2$ is the total cumulative frequency of MN-PCEs; exp is the exponential function; $x$ is the time of the process; $x_o$ is the middle of the curve; and d$x$ is the width of the curve.

The initial time ($T_i$) and final time ($T_f$) corresponding to the time required for the MN-PCEs to achieve an accumulation of 4% and the time at which the slope of the kinetic curve becomes essentially constant, respectively, were determined from the adjusted curves. The maximal rate ($V_{max}$) of micronucleated cell production was also calculated. These calculations were performed using a program that was developed using the C programming language in our laboratory.

The time of maximal induction ($T_{max}$) was determined by adjusting the curve of MN-PCE induction as a function of time using the spline tool of the Microcal Origin PC program version 6 (Microsoft). The time of relative maximal induction ($T_{rmi}$) for the chemical mutagens was determined by subtracting $T_{max}$ of 0.25-Gy gamma radiation [16] from the Tmax of the chemical agent. Radiation was used as a reference, because it does not have to be absorbed, metabolized, or distributed to cause DNA breaks.

### Genotoxicity

The genotoxicity of the different treatments was calculated as using the area beneath the curve (ABC) of MN-PCE induction vs time, and the genotoxic capacity (GC) was established as the ABC with respect to the dose in µmoles per kg of body weight.

### Cytotoxicity

The cytotoxicity of the different treatments was calculated as the maximum reduction in the PCE frequency (percentage) from the curve of PCE frequency vs time with respect to the frequency prior to treatment (0 h). The cytotoxic capacity (CC) was defined as the maximal cytotoxicity with respect to the dose in µmol per kg of body weight.

### Statistics

Samples collected prior to dFdC administration from each mouse could be used as the corresponding controls, thereby allowing for statistical comparisons with the control through paired $t$ tests, with significance set at $p < 0.05$. The use of these samples as controls increased the statistical power by reducing the random variation between animals. The statistical comparisons were performed using Microsoft Excel (Office).

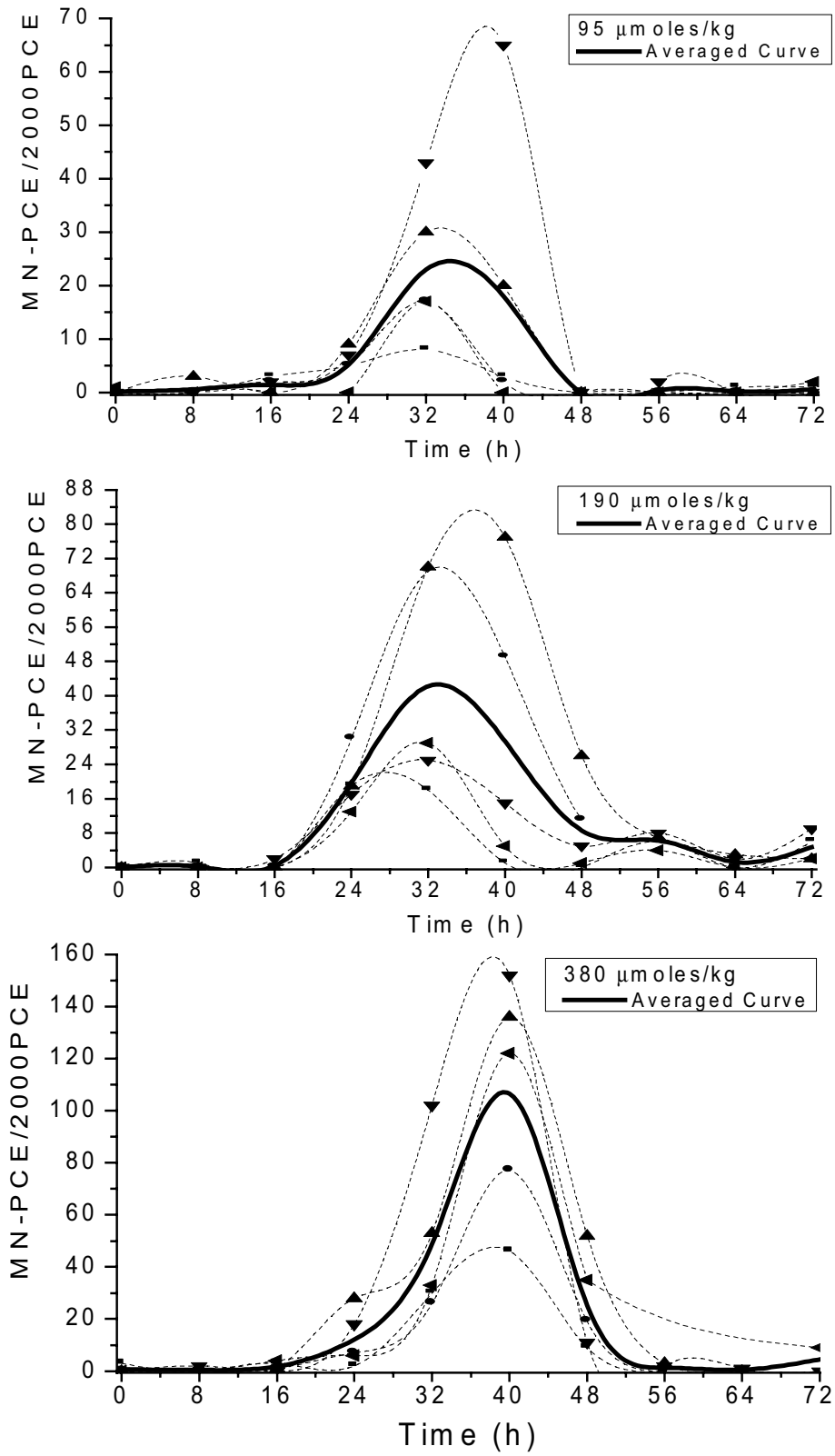


**Fig. 1** Time-course curve of the frequency of MN-PCEs in murine peripheral blood in response to different doses of dFdC. The individual curves for five mice from each group as well as the average curves were plotted. The timings of the maximum induction obtained with the doses of 95, 190, and 380 µmol/kg were 34.2, 32.7, and 40 h, respectively. The *text* indicates that the points were significantly different from the control (paired *t* test)

## Results

The individual and average time-course curves of MN-PCE induction following exposure to different doses of dFdC are shown in Fig. 1. The average curves were symmetric, and the doses of 95 and 190 µmol per kg of body weight resulted in a maximum induction of MN-PCEs at 34.2 and 32.7 h post-treatment, respectively. The dose of 380 µmol/kg delayed MN-PCE induction by 5.8 and 7.3 h with respect to the lower doses, and maximal induction occurred approximately 40 h post-treatment. All doses presented responses with high variability. Because the dose of 380 µmol/kg resulted in high levels of cell death, the frequency of MN-PCEs was determined using fewer than 2000 PCEs per animal in certain cases: $701 \pm 73$ PCEs at 40 h, $316 \pm 73$ PCEs at 48 h, and $1409 \pm 742$ PCEs at 56 h. In addition, two mice died 64 h post-treatment, and another mouse died 72 h after receiving the dose of 380 µmol/kg. The paired $t$ test ($p < 0.05$) was used to compare the data from each animal at different times to the data obtained at 0 h, which was used as a control. Statistical analyses indicated that the lowest dose caused significant differences at 24 and at 32 h, the dose of 190 µmol/kg of body weight caused significant differences from 24 to 56 h and the highest dose caused significant differences from 16 to 48 h. The average basal frequency obtained from the control (0 h) data was $2.2 \pm 0.67$ MN-PCEs per 2000 PCEs.

Figure 2 shows graphs depicting the dFdC dose as a function of the area under beneath the curve (ABC) of the time course of MN-PCE induction and as a function of the maximum MN-PCE induction. The correlation coefficients for these graphs were 0.994 and 0.995, respectively. Both parameters of MN-PCE induction were directly proportional to the dose, although the ABC appears to be a more suitable index, because it represents an index of total MN-PCE induction.

The genotoxic capacity (GC) of dFdC, which is defined as the ABC of MN-PCE induction as a function of time per dose (µmol/kg), was 5.26. The ranges of this parameter for 12 previously studied agents varied by in terms of the order of magnitude from 2.3 to approximately 15,000 [9], which implied that dFdC is not particularly active as a inducer of DNA breaks and micronuclei.

Additional parameters were established by comparing the results of the present study with previously reported findings on treatments with different agents in the same system. One such parameter is the difference in $T_{max}$ of a chemical agent with respect to $T_{max}$ of gamma ray kinetics. This parameter, which is defined as the time of relative maximal induction ($T_{rmi}$), allows us to infer the time required for the agent of interest to induce the maximum number of MNs resulting from either DNA breaks or chromosomes. Agents that require metabolic activation or induce DNA breaks through complex processes require more time than those that simply cause DNA damage and breaks during repair [17]. Figure 3 shows the $T_{rmi}$ values for agents with different mechanisms of action compared with the $T_{rmi}$ for dFdC. The data for different agents represent our previously published data for the lowest dose of an agent administered under the same conditions. The lowest doses were used to minimize the cytotoxic effects of certain agents, which caused a delay in MN-PCE induction,

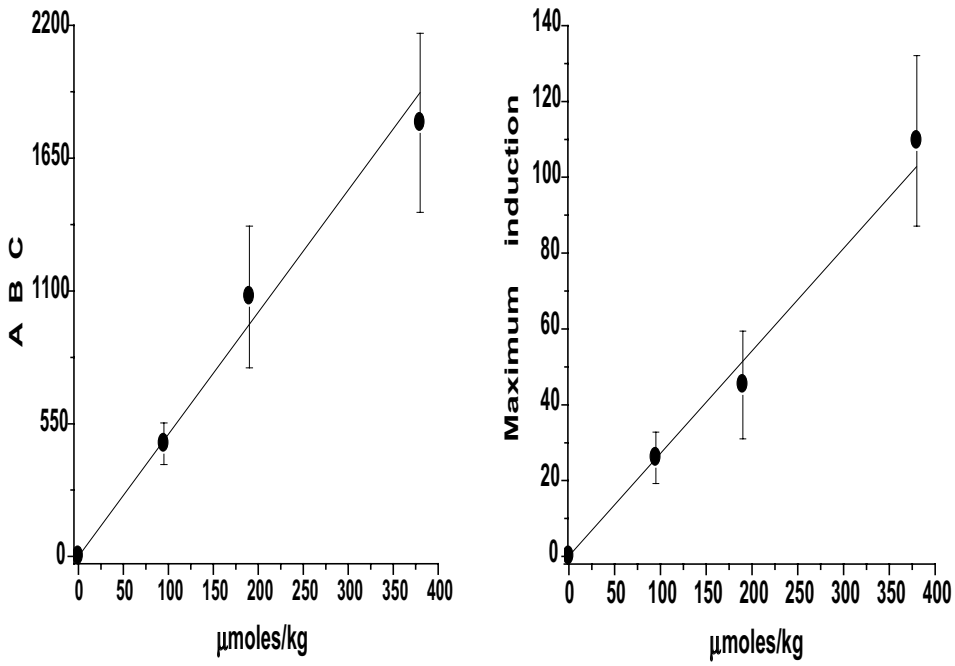


**Fig. 2** Curves of the dFdC dose as a function of the area beneath the curve (ABC) of the time course for MN-PCE induction and as a function of the maximal induction. *Both curves* indicate a direct correlation between the MN-PCE levels and dFdC dose

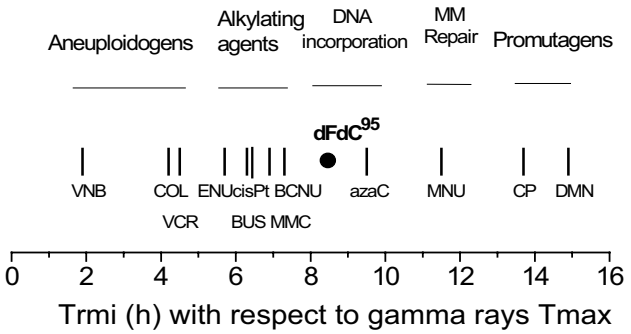


**Fig. 3** $T_{rmi}$ for agents with different mechanisms of action (*bars*) compared with $T_{rmi}$ of dFdC (*point*). The data from different agents represent our previously published data, which were obtained using the lowest dose tested under the same conditions and showed a reduction in maximal PCE between 23 and 57% [8]. The data used for the comparison were obtained at the lowest dFdC dose (95 µmol/kg)

thus increasing $T_{rmi}$ [9]. We also compared only the data obtained from the lowest dose of dFdC (95 µmol/kg), and the results indicated that micronuclei induction by dFdC has $T_{rmi}$ of 8.5 h. This time is longer than the values obtained for aneugens (1.9–4.5 h), which induce MN-PCEs by disrupting the mitotic spindle, and alkylating agents (5.7–7.3 h), which cause DNA breaks but have $T_{rmi}$ values that are shorter than those caused by agents that induce DNA breaks via complex processes, such as azaC and methylnitrosourea, which have $T_{rmi}$ values of 9.5 and 11.5 h, respectively [9].

The cytotoxicity curves measured based on the PCE frequencies, which are shown in Fig. 4, indicate that dFdC is highly toxic. The dose of 95 µmoles/kg of body weight (Fig. 4a) reduced the average PCE levels by approximately 80% at 39.2 h post-treatment. However, this effect was reversible at 65 h post-treatment, at which point the PCE level returned to that observed before treatment. Treatment with 190 µmol/kg of body weight (Fig. 4b) caused a very heterogeneous response. Therefore, individual data were plotted; two animals showed marked PCE induction after 40 h and exhibited values that were four and eightfold higher than the original PCE frequency. One animal showed a response similar to that obtained using 95 µmol/kg of body weight, and two other animals showed a response similar to that obtained using 380 µmol/kg of body weight (Fig. 4c). The highest dose caused a reduction in the PCE frequency of approximately 95%, and this frequency reduction was not recovered by the end of the experiment. These results suggest that a dose of 190 µmol/kg of body weight falls within a transitional region of the dose–response relationship in terms of cytotoxicity. Paired *t* tests were used to compare the data at different timepoints with respect to the control (time 0). The results are as follows: 95 µmol per kg of body weight caused significant differences ($p < 0.05$)

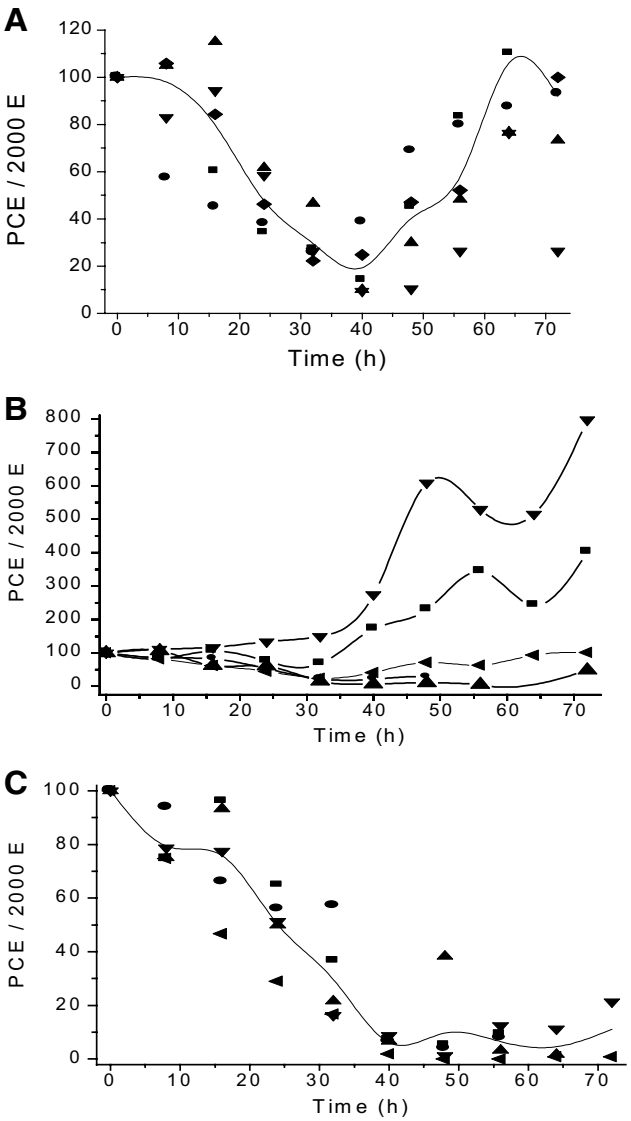


**Fig. 4** Time course of cytotoxicity as measured by the PCE levels with different dFdC doses. The effect of the 95 µmol/kg dose on the PCE frequency is plotted in **a**. The *points* represent individual values, and the *curve* represents the average curve. The *curve* indicates that the maximal toxic effect observed at 40 h was reversible by the end of the experiment (72 h). For the 190 µmol/kg dose, the individual responses were plotted (**b**), because the responses were variable, with a reversible effect and erythropoiesis induction observed in certain mice and an irreversible effect observed in other mice. The 380 µmol/kg dose (**c**) caused an irreversible decrease in the PCE levels, with the *points* representing individual values and the *curve* representing average *curves*

from 8 to 56 h, the dFdC dose of 190 µmol per kg causes significant difference at any time as a result of dispersion, and 380 µmol per kg of body weight caused significant differences from 8 to 56 h.

The maximal cytotoxicity and genotoxicity were observed at approximately the same times for the dFdC dose of 95 µmol/kg, suggesting that these two events are

related. Because the cytotoxic responses were completely reversed within the study period, the genotoxicity kinetics could be compared with the cytotoxicity kinetics by plotting the cumulative frequencies and adjusting the curves to the Boltzmann equation as described in "Methods". The curves of the cumulative frequencies for genotoxicity and cytotoxicity induced by the dFdC dose of 95 μmoles/kg are shown in Fig. 5. These curves indicate that the two parameters have different kinetics. The curves of genotoxicity and cytotoxicity fit the Boltzmann curve with an $r$ value of 0.99. The kinetic parameters of the curves of genotoxicity and cytotoxicity for the group of five mice treated with 95 μmol/kg dFdC are compared in Table 1. Cytotoxicity occurred earlier and persisted longer than genotoxicity. This observation can also be analyzed numerically by comparing the data from this figure with those shown in Table 1. The Ti value for cytotoxicity obtained for the dose of 95 μmol/kg was 9.8 h, whereas the corresponding $T_i$ value for genotoxicity was 19.6 h. The $T_f$ value for genotoxicity obtained for the dose of 95 μmol/kg was 51.9 h, whereas the $T_f$ value for cytotoxicity was 75.4 h. These results demonstrate that cytotoxicity was initiated earlier and persisted longer than genotoxicity.

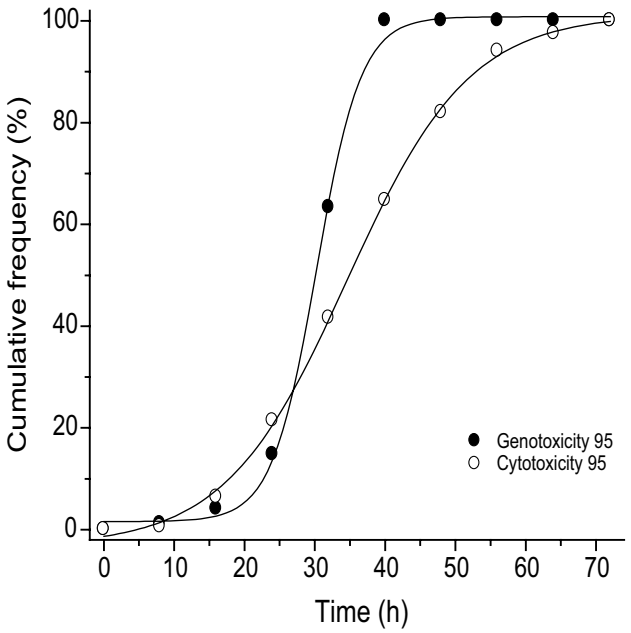


**Fig. 5** Cumulative frequency curves for the genotoxicity and cytotoxicity induced by the dFdC dose of 95 μmol/kg. The kinetics of genotoxicity were compared with the kinetics of cytotoxicity by plotting the cumulative frequencies and adjusting the curves to the Boltzmann equation ($r=0.99$), as described in "Methods". These *curves* indicate that the two events have different kinetics

## Discussion

Gemcitabine, or dFdC, is a nucleotide analog that exhibits antineoplastic properties in different types of cancer [18–20]. The activity of dFdC operates through two routes of action: its effects on nucleotide metabolism prior to its incorporation and its effects on enzymes involved in DNA synthesis and repair after its incorporation. As a result, after the transporter-dependent internalization of dFdC [21], this nucleotide analog inhibits ribonucleotide reductase, thereby decreasing the deoxynucleotide pools and increasing the probability of its incorporation [22]. A recent study showed that dFdC and 2′,2′-difluoro-2′-deoxyuridine (dFdU), a deamination product of dFdC, inhibit thymidylate synthase [23], an enzyme that catalyzes the synthesis of dTMP and whose inhibition causes dTMP deficiency and cell death. The other route implies that dFdC is phosphorylated to form its triphosphate derivative and incorporated into DNA [24]. An in vitro assay showed that (i) dFdC 5′-triphosphate and deoxycytidine triphosphate competed for incorporation into the C sites of the growing DNA strand; (ii) dFdC triphosphate is incorporated into DNA, although at one deoxynucleotide after dFdCMP incorporation, the polymerization process was interrupted; and (iii) polymerase epsilon did not excise dFdCMP from the 3′-terminus of DNA primers [25]. In addition, evidence was obtained that dFdC inhibited topoisomerase I [26].

Our results indicate that all dFdC doses caused a single-peak curve of MN-PCE induction plotted as a function of time. The number of peaks is the first indication of the involvement of one or more mechanisms. As shown in Fig. 6, bis-chloroethylnitrosourea (BCNU) had one peak and a shoulder, suggesting two mechanisms. If two peaks are not clearly observed, the broadness of the curve indicates superposed curves as well as the possibility of micronuclei induction by more than one mechanism as shown

**Table 1** Kinetic parameters of the curves induction and PCE reduction caused diflurodeoxycytidine

| | Dose (μmol/kg) bw | *Ti* (h) | *T*max (h) | *T*f (h) | *V*max | Fit Boltzman (*r*) | *n* |
|---|---|---|---|---|---|---|---|
| MN-PCE (genotoxicity) | 95 | 19.6 | 34.2 | 51.9 | 7.6 | 0.99834 | 5 |
| PCE (cytotoxicity) | 95 | 9.8 | 34 | 75.4 | 3.1 | 0.99935 | 5 |

*Ti* initial time, $T_{max}$ time maximum induction, *Tf* final time, *Vmax* maximal velocity, *n* number animals

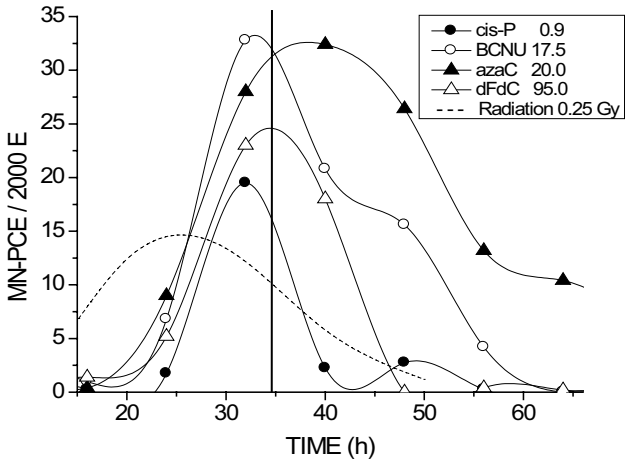


**Fig. 6** Comparison of the frequency of MN-PCEs as a function of time after a single exposure to different agents, including gamma rays. The curves represent the average curves from five mice as a function of the indicated dose (in μmol/kg of body weight). The data were obtained from our previous studies under the same conditions used in the present study [8, 27, 40]. *cisPt* platinum (II) diaminochloride, *BCNU* bis-chloroethyl nitrosourea, *azaC* 5-azacytidine, *dFdC* 2′,2′-difluoro-2′-deoxycytidine, *radiation* gamma rays

by the average curve (Fig. 6) obtained from the individual curves of the five mice treated with azaC. The individual curves (not shown) clearly displayed two peaks [27]. In this case, the following index of curve broadness (BI) could be used: ABC/maximal induction, i.e., the area beneath the curve of MN-PCE induction as a function of time divided by the maximal induction. These BIs for BCNU and azaC were 27.1 and 34.3, respectively [9]. The BI index for dFdC was found to equal 14.3, and this value is unique among the 12 previously assayed agents, which exhibited a slightly higher index than cis-Pt (BI 13) [9]. The presence of a single peak in the curve of MN-PCE induction as a function of time and its low BI indicates that dFdC induces DNA breaks either by a single mechanism or by mechanisms that occur concomitantly. By comparing the responses of the two previously studied analogs of cytidine, i.e., azaC and dFdC, we observed that the complexity of the kinetics of MN-PCE induction appears to be related to differences in the complexity of the reported mechanisms of action involved in DNA break formation. dFdC appears to cause DNA breaks as a result of blocking DNA synthesis by the concomitant inhibition of polymerases and topoisomerase, whereas azaC causes (i) DNA mega-adduct, by a covalent link between DNA and DNA-cytosine methyltransferase [28], (ii) the subsequent intent of the cell to repair this lesion by different mechanisms, (iii) the inhibition of the methylation process, and (iv) finally, the consequences of demethylation on DNA fragility [29].

The time required for different agents to induce MN-PCEs could be related to the mechanisms of micronuclei induction. The difference in $T_{max}$ of an agent with respect to $T_{max}$ of ionizing radiation ($T_{rmi}$) is a good index for the action of several groups of agents [9]. Aneuploidogens presented low average $T_{rmi}$ of $3.5 \pm 1.4$ h, which is likely because these agents act during the last step of MN-PCE induction, whereas mono- and bifunctional alkylating agents showed a difference of $6.5 \pm 0.6$ h, the micronuclei resulting from DNA breaks during repair. Alkylating agents which require metabolic activation in the liver showed $T_{rmi}$ of $14.3 \pm 0.8$ h. Methylnitrosourea, with which has $T_{rmi}$ of 11.5 h, did not fit within these two groups of alkylating agents, which may be related to the generation of DNA breaks during mismatch repair during the second division after exposure as previously reported [10]. Moreover, the average curve for azaC showed $T_{rmi}$ of 9.5 h; however, the individual curves clearly showed two peaks at 8.4 and 21.8 h [25]. Two previously reported factors appear to determine $T_{rmi}$ for this agent: the requirement of incorporation into DNA and the repair of the mega-adduct generated during the methylation of DNA substituted with azaC by a covalent bond formed between the substituted DNA and DNA methyltransferase [28]. The results of the present study indicated that $T_{rmi}$ of dFdC was 8.5 h, and this value is similar to the value of 8.4 h corresponding to the first peak of azaC, which has been reported to require DNA incorporation and inhibit the initiation of DNA synthesis [30] despite representing a good substrate for DNA polymerase alpha [31]. Studies with more well-known antimetabolites are required to better understand the correlation between the kinetics of micronuclei induction and the confirmed mechanisms of action. As a result, DNA breaks and micronuclei induction by dFdC appears to be dependent on its prior incorporation into DNA [24], a finding that could be explained by the previously reported inhibition of DNA polymerase alpha, polymerase epsilon [25], and/or topoisomerase I [26] by dFdC. Thus, the ability of dFdC to inhibit ribonucleotide reductase [22] and thymidylate synthase [23] prior to its incorporation into DNA is not involved in the genotoxic effect but is probably involved in the cytotoxic effect.

The cytotoxicity of dFdC was previously reported to be related to the induction of apoptosis [32]. We observed that the lowest dose used in the present study caused a reversible cytotoxic effect. The maximal reduction of PCEs occurred at 40 h, although the PCE frequency had almost returned to the basal frequency by the end of the experiment (72 h). This observation could be explained by the homeostatic response of bone marrow to erythrocyte reduction, an erythropoietic response that is characterized by the involvement of complex molecular processes [33]. This effect appears to be enhanced with the dose of 190 μmol/kg, which resulted in a higher recovery compared with the basal values in some mice. This effect is likely the result of

a combination of erythrocyte reduction caused by the toxicity of dFdC toward bone marrow and the subsequent stimulation of erythropoiesis. The results indicate that dFdC is cytotoxic, although this effect could be reverted by cell proliferation of non- or low-damaged cells depending on the dose.

The time of maximal cytotoxicity was 34 h, which is correlated with the time of maximal genotoxicity, thus suggesting a correlation between cytotoxicity and micronuclei induction. This observation is consistent with previous in vitro studies that suggested a causal relationship between the induction of DNA breaks and cytotoxicity [34]. However, the comparison of cytotoxicity and genotoxicity kinetics induced by the lowest dose indicated that cytotoxicity is initiated earlier at 9.8 h and ends later at 75.4 h relative to genotoxicity, which is initiated at 19.6 h and ends at 54.9 h. These results suggest that although cell toxicity appears to be mainly related to DNA break induction, at least one additional mechanism is responsible for early and late cell toxicity. The mechanisms that cause early cytotoxicity could occur prior to dFdC incorporation into DNA, such as the previously reported inhibition of thymidylate synthase [23] and/or ribonucleotide reductase [22].

In addition, evidence indicates that certain effects induced by dFdC are dependent on an increase in the levels of reactive oxygen species (ROS), suggesting that dFdC induces ROS production [35, 36]. These data suggest that dFdC induces early cell damage, including DNA damage, via cytotoxic effects instead of long-lasting genotoxic effects, i.e., lethal non-repairable DNA lesions.

In vivo analyses of MN-PCE induction over time permit the establishment of strong indexes of the genotoxic and cytotoxic capacities of an agent [37]. The results indicated that the MN-PCE frequency was proportional to the dose as measured by both the maximal frequency and the ABC of MN-PCE induction as a function of time. The latter parameter is a strong index of genotoxic activity, because it reflects the total MN-PCE induction. We proposed a robust index of GC that correlates with the ABC per μmol to consider the mass of the molecule that is being studied. In a previous study, we found that the GC varies by orders of magnitude [9]. In addition, this large variation is consistent with the results of previous in vitro genotoxic studies [38]. The agents with higher GC values were aneugens, which had a GC of $365 \pm 33$, followed by alkylating agents, which showed high variability and a GC of $155 \pm 195$, and promutagens, which had a GC of $4.2 \pm 2.2$; these groups of agents had $T_{rmi}$ values of $3.5 \pm 1.4$, $6.5 \pm 0.6$, and $14.3 \pm 0.8$ h, respectively. These findings suggest that an inverse relationship occurred between the GC and the time required for inducing MN-PCE [9]. The GC for dFdC was 5.26, suggesting that this agent was not particularly efficient in molar terms and its mechanism for inducing micronuclei requires a long amount of time as indicated by its $T_{rmi}$ of 8.5 h. These findings are consistent with the possibility that the action of dFdC is dependent on its prior incorporation into DNA [24], where it inhibits DNA polymerases and topoisomerase [25, 26].

With respect to cytotoxic capacity (CC), the lowest dFdC dose exhibited a CC of 0.8 (in μmol/g), which was measured as the maximal reduction of PCEs with respect to the dose. This CC was lower than the results obtained for other agents, which exhibited CCs varying from 0.1 to almost 900 [8]. Aneuploidogens showed an average CC of $368 \pm 458$, and alkylating agents showed an average CC of $6.5 \pm 11.2$. These results indicate that the GC of dFdC is low in molar terms.

The present study forms part of an inductive process that aims to correlate previous observations reported in the literature at the cellular and molecular levels with the kinetic induction of genotoxic and cytotoxic effects of different agents. Although the establishment of generalities in the future will require many more studies, the results obtained in the present investigation appear to support this possibility. This strategy could contribute to the establishment of an in vivo approach that allows for the use of MN-PCE induction kinetics to infer the probable genotoxic action of antineoplastic agents. In addition, this approach could be used as a screening method during the development of potential antineoplastic agents and could even contribute to the establishment of novel therapeutic protocols based on the time of action after treatment with antineoplastic agents. Assessing the kinetics of MN-PCE induction could be simplified via flow cytometry [39].

The results obtained allow us to draw the following conclusions:

1. dFdC induces MN-PCE induction in proportion to the dose.
2. dFdC induces DNA breaks via a single mechanism or concomitant mechanisms.
3. $T_{rmi}$ of dFdC was higher than that of aneuploidogens and alkylating agents, suggesting that micronuclei induction by dFdC is dependent on its prior incorporation into DNA; this finding is likely related to the previously reported inhibitory effect of dFdC on DNA polymerase alpha, polymerase epsilon [25], and/or topoisomerase I [26].
4. The timing of maximal cytotoxicity is correlated with the timing of maximal genotoxicity, suggesting a correlation between cytotoxicity and micronuclei induction.
5. The results revealed the occurrence of early cytotoxic effects that were unrelated to the genotoxic effect and independent of dFdC incorporation into DNA, which according to the literature, could be caused by the inhibition of thymidylate synthase [23] and/or ribonucleo-

tide reductase [22] or by the reported induction of ROS by dFdC [35, 36].

6. The genotoxic and cytotoxic capacities of dFdC are low compared with those of aneugens and direct alkylating agents, which were previously studied in the same system [9].

**Acknowledgements** We would like to thank Angel Reyes and Perfecto Aguilar for providing excellent technical assistance.

**Compliance with ethical standards**

**Animal welfare** The animals were treated and housed in accordance with the Guide for the Care and Use of Laboratory Animals, Commission on Life Sciences, Institute of Laboratory Animal Research, National Research Council (1996). The protocol was reviewed and approved by the Internal Committee of Care and Use of Laboratory Animals (CICUAL) that oversees the ethics of research involving the use and welfare of animals.

**Funding** This work was supported by Project CB-507 from the Instituto Nacional de Investigaciones Nucleares (México) and Project 240116 from the Consejo Nacional de Ciencia y Tecnología (CONACYT) of México.

## References

1. Serdjebi C, Milano G, Ciccolini J (2015) Role of cytidine deaminase in toxicity and efficacy of nucleosidic analogs. Expert Opin Drug Met Toxicol 11:665–672.
2. Lawley PD, Phillips DH (1996) DNA adducts from chemotherapeutic agents. Mutation Res 355:13–40.
3. Parker PW (2009) Enzymology of purine and pyrimidine antimetabolites used in the treatment of cancer. Chem Rev 109:2880–2893
4. Crespan E, Garbelli A, Amoroso A, Maga G (2011) Exploiting the nucleotide substrate specificity of repair DNA polymerases to develop novel anticancer agents. Molecules 16:7994–8019
5. Li KK, Li F, Li QS, Yang K, Jin B (2013) DNA methylation as a target of epigenetic therapeutics in cancer. Anticancer Agents Med Chem 13:242–247
6. Ferrara R, Pilotto S, Peretti U, Caccese M, Kinspergher S, Carbognin L, Karachaliou N, Rosell R, Tortora G, Bria E (2016) Tubulin inhibitors in non-small cell lung cancer: looking back and forward. Expert Opin Pharmacother 17:1113–1129
7. Lee JJ, Huang J, England CG, McNally LR, Hermann B, Frieboes HB (2013) Predictive modeling of in vivo response to gemcitabine in pancreatic cancer. PLoS One 9:e1003231.
8. Morales-Ramírez P, Vallarino-Kelly T, Anguiano-Orozco G, Rodríguez-Reyes R (1997) Pharmacokinetic parameters of genotoxic activity inferred by the comparison of the kinetics of MN-PCE induced by chemical agents and ionizing radiation. Mutation Res 391:127–134.
9. Morales-Ramírez P, Vallarino-Kelly T, Cruz-Vallejo V (2014) Kinetics of micronucleus induction and cytotoxicity caused by distinct antineoplastics and alkylating agents in vivo. Toxicol Lett 224:319–325
10. Armstrong MJ, Galloway SM (1997) Mismatch repair provokes chromosome aberrations in hamster cells treated with methylating agents or 6-thioguanine, but not with ethylating agents. Mutation Res 373:167–178.
11. Aydemir N, Bilaloglu R (2003) Genotoxicity of two anticancer drugs, gemcitabine and topotecan, in mouse bone marrow in vivo. Mutation Res 537:43–51.
12. Classen J, Paulsen F, Hehr T, Bamberg M, Budach W (2002) Effect of gemcitabine on acute and late radiation toxicity of skin and underlying soft tissues to single-dose irradiation in a nude mice model. Int J Radiat Oncol Biol Phys 53:197–205
13. Grégoire V, Beauduin M, Rosier JF, De Coster B, Bruniaux M, Octave-Prignot M, Scalliet P (1997) Kinetics of mouse jejunum radiosensitization by 2′,2′-difluorodeoxycytidine (gemcitabine) and its relationship with pharmacodynamics of DNA synthesis inhibition and cell cycle redistribution in crypt cells. Br J Cancer 76:1315–1321
14. Viveka S, Udyavar A, Shetty B, Kuriakose S, Sudha MJ (2015) Histomorphometric effects of gemcitabine on Swiss albino mice spermatogenesis. Adv Biomed Res 4:29–34
15. Schmid W (1975) The micronucleus. Mutation Res 31:9–15.
16. Morales-Ramírez P, Vallarino-Kelly T (1998) Pharmacokinetic parameters determined from the clastogenic activity of ethylnitrosourea (ENU) and dimethylnitrosamine (DMN) in mice in vivo. Mutation Res 412:315–322.
17. Erlichman C (1987) The pharmacology of anticancer drugs. In: Tannock IF, Hill RP (eds) The basic science of oncology. Pergamon Press, USA, pp 292–307
18. Braakhuis BJ, van Dongen GA, Vermorken JB, Snow GB (1991) Preclinical in vivo activity of 2,2-difluorodeoxycytidine (gemcitabine) against human head and neck cancer. Cancer Res 51:211–214
19. Grunewald R, Kantarjian H, Du M, Faucher K, Tarassoff P, Plunkett W (1992) Gemcitabine in leukemia: a phase I clinical, plasma, and cellular pharmacology study. J Clin Oncol 10:406–413
20. Noble S, Goa KL (1997) Gemcitabine. A review of its pharmacology and clinical potential in non-small cell lungcancer and pancreatic cancer. Drugs 54:447–472
21. Mackey JR, Mani RS, Seiner M, Mowles D, Young JD, Belt JA, Crawford CR, Cass CE (I998) Functional nucleoside transporters are required for gemcitabine influx and manifestation of toxicity in cancer cell lines. Cancer Res 58:4349–4357
22. Heinemann V, Xu YZ, Chubb S, Sen A, Hertel LW, Grindey GB, Plunkett W (1990) Inhibition of ribonucleotide reduction in CCRF-CEM cells by 2′,2′-difluorodeoxycytidine. Mol Pharmacol 38:567–572
23. Honeywell RJ, Ruiz van Haperen VW, Veerman G, Smid K, Peters GJ (2015) Inhibition of thymidylate synthase by 2′,2′-difluoro-2′-deoxycytidine (Gemcitabine) and its metabolite 2′,2′-difluoro-2′-deoxyuridine. Int J Biochem Cell Biol 60:73–81
24. Veltkamp SA, Pluim D, van Eijndhoven MAJ, Bolijn MJ, Ong FHG, Govindarajan R, Unadkat JD, Beijnen JH, Schellens JHM (2008) New insights into the pharmacology and cytotoxicity of gemcitabine and 2′,2′-difluorodeoxyuridine. Mol Cancer Ther 7:2415–2425
25. Huang P, Chubb S, Hertel LW, Grindey GB, Plunkett W (1991) Action of 2′,2′-difluorodeoxycytidine on DNA synthesis. Cancer Res 51:6110–6117
26. Pourquier P, Gioffre C, Kohlhagen G, Urasaki Y, Goldwasser F, Hertel LW, Yu S, Pon RT, Gmeiner WH, Pommier Y (2002) Gemcitabine (2′,2′-difluoro-2′-deoxycytidine), an antimetabolite that poisons topoisomerase I. Clin Cancer Res 8:2499–2504
27. Morales-Ramírez P, Vallarino-Kelly T, Cruz-Vallejo VL (2008) Mechanisms of DNA breaks induction in vivo by 5-azacytidine: paths of micronucleus induction by azaC. J Appl Toxicol 28:254–259
28. Santi DV, Norment A, Garret CE (1984) Covalent bond formation, between a DNA-cytosine methyltransferase and DNA containing 5-azacytosine. Proc Natl Acad Sci USA 81:6993–6997

29. Satoh T, Yamamoto K, Miura KF, Sofuni T (2004) Region-specific chromatin decondensation and micronucleus formation induced by 5-azacytidine in human TIG-7 cells. Cytogenet Genome Res 104:289–294
30. Tobey RA (1972) Effects of cytosine arabinoside, daunomycin, mithramycin, azacytidine, adriamycin, and camptothecin on mammalian cell cycle traverse. Cancer Res 32:2720–2725
31. Bouchard J, Momparler RL (1983) Incorporation of 5-aza-2′-deoxycytidine-5′-triphosphate into DNA. Interactions with mammalian DNA polymerase alpha and DNA methylase. Mol Pharmacol 24:109–114
32. Giovannetti E, Mey V, Loni L, Nannizzi S, Barsanti G, Savarino G, Ricciardi S, Del Tacca M, Danesi R (2007) Cytotoxic activity of gemcitabine and correlation with expression profile of drug-related genes in human lymphoid cells. Pharmacol Res 55:343–349
33. Brenet F, Kermani P, Spektor R, Rafii S, Scandura JM (2013) TGFβ restores hematopoietic homeostasis after myelosuppressive chemotherapy. J Exp Med 210:623–639
34. Auer H, Oehler R, Lindner R, Kowalski H, Sliutz G, Orel L, Kucera E, Simon MM, Glössl J (1997) Characterisation of genotoxic properties of 2′,2′-difluorodeoxycytidine. Mutation Res 393:165–173.
35. Donadelli M, Constanzo C, Beghelli S, Scupoli MT, Dandrea M, Bonora A, Piacentini P, Budillon A, Caraglia M, Scarpa A, Palmieri M (2007) Synergistic inhibition of pancreatic adenocarcinoma cell growth by trichostatin A and gemcitabine. Biochim Biophys Acta 1773:1095–1106.
36. Maehara S, Tanaka S, Shimada M, Shirabe K, Saito Y, Takahashi K, Maehara Y (2004) Selenoprotein P, as a predictor for evaluating gemcitabine resistance in human pancreatic cancer cells. Int J Cancer 112:184–189
37. Morales-Ramírez P, Vallarino-Kelly T, Rodríguez-Reyes R (1996) Effect of chlorophyllin on gamma ray induced micronuclei in polychromatic erythrocytes of murine peripheral blood determined by the ABC strategy. Mutation Res 367:51–56.
38. Perry P, Evans HJ (1975) Cytological detection of mutagen-carcinogen exposure by sister chromatid exchange. Nature 258:121–125
39. Abramsson-Zetterberg L, Grawé J, Zetterberg G (1995) Flow cytometric analysis of micronucleus induction in mice by internal exposure to 137Cs at very low dose rates. Int J Radiat Biol 67:29–36
40. Morales-Ramírez P, Vallarino-Kelly T, Cruz-Vallejo VL, López-Iturbe R, Alvaro-Delgadillo H (2004) In vivo kinetics of micronuclei induction by bifunctional alkylating antineoplastics. Mutagenesis 19:207–213